Kinetics of Pyrolysis of Durian (*Durio zibethinus* L.) Shell Using Thermogravimetric Analysis

Yee Ling Tan,[1] Muthanna J. Ahmed,[2] Esam H. Hummadi[3] and Bassim H. Hameed[1*]

[1]School of Chemical Engineering, Universiti Sains Malaysia,
Engineering Campus, 14300 Nibong Tebal, Pulau Pinang, Malaysia

[2]Chemical Engineering Department, Engineering College, Baghdad University,
P.O. Box 47024, Aljadria, Baghdad, Iraq

[3]Department of Biotechnology, College of Science, University of Diyala,
P.O. Box 33, Baqubah, Iraq

*Corresponding author: chbassim@usm.my

ABSTRACT: *The characteristics and kinetics of durian shell (DS) pyrolysis were investigated using non-isothermal thermogravimetric analysis (TGA). DS is a cellulose-rich biomass with high volatile matters content, which is suitable for bio-oil production. Thermal decomposition experiments were performed under nitrogen flow at various heating rates (i.e., 5°C min⁻¹, 10°C min⁻¹ and 20°C min⁻¹). The model-fitting method represented by Coats-Redfern was applied on the experimental TGA data of DS pyrolysis. The decomposition of DS was divided into three stages: first stage (59°C–200°C) involved removal of moisture and light volatiles; second stage (200°C–400°C) showed decomposition of cellulose and hemicellulose; and third stage (above 400°C) presented lignin decomposition. There was 56% weight loss observed in second stage, revealing that decomposition of cellulose and hemicellulose contributed the most on volatile production. The model shows that the activation energy was between 42.08 kJ mol⁻¹ and 84.40 kJ mol⁻¹ for the second stage of the pyrolytic process from 200°C to 400°C using different decomposition mechanisms. The Coats-Redfern method is applied successfully for the correlation of experimental TGA data with an average correlation coefficient (R^2) of 0.991 while one-way diffusion model D1 gave the highest correlation coefficient of 0.998. DS biomass is a suitable raw material for energy or chemicals production.*

Keywords: Kinetics, pyrolysis, thermogravimetric analysis, durian shell, biomass

1.   1. INTRODUCTION

Researchers have been evaluating the utilisation of biomass from agricultural and animal wastes as a renewable source for fuels and chemicals due to its favourable properties in terms of potential energy.[1–5] Biochemical, physiochemical and thermochemical processes are used for this purpose, with the dominance on the latter method because of its effectiveness in the thermal decomposition of biomass to volatiles and char products.[6] The most developed thermochemical techniques are pyrolysis, gasification and combustion.[7–10]

Among the thermal decomposition processes, pyrolysis is the most effective and widely adopted method in converting organic compounds into useful products under an inert atmosphere and relatively low temperatures. During pyrolysis, the main products are light gases (volatiles), liquids (bio-oil) and solid char.[11] Both light gases and bio-oil products are effective fuel sources because of their high heating values.[12] Bio-oil also contains various organic compounds, which can be used as feedstock for value-added products.[13]

Both decomposition behaviour and kinetics should be investigated to determine the most suitable design and operation of pyrolytic process.[14] Thermogravimetric analysis (TGA) is the most common and simplest method of evaluating the kinetics of pyrolysis.[15–17] The TGA determines the weight loss during sample decomposition as a function of time or temperature under inert atmosphere at a constant heating rate.[18]

Pyrolysis kinetics can be analysed under isothermal or non-isothermal conditions. The major drawback of the isothermal method is sample loss before rising to the required temperature, causing a specific error during analysis. Thus, non-isothermal TGA is more accurate in the evaluation of kinetic parameters by using either model-fitting or model-free methods.[19] The first method estimates the kinetic parameters based on prior assumptions of the reaction mechanism model.[20] The activation energy in the model-fitting method is calculated at various heating rates and temperatures without a reaction function.[21] The non-isothermal TGA method has been widely applicable in the kinetic analyses of different biomass pyrolyses such as corn straw, karanj fruit hulls, rice husk, smooth cordgrass, hazelnut husk and *Hydrilla verticillata*.[14,22–24,25,26]

Durian (scientific name *Durio zibethinus* L.; family Bombacaceae), is a seasonal fruit that is most popular in Southeast Asia, particularly in Malaysia, Indonesia, Thailand and the Philippines.[27] The tree grows up to 40 m in height with a typical buttressed trunk and 3–7 cm long oblong or elliptical dark green leaves.[28] The fruit

is oval-shaped with a weight of 2–4.5 kg based on its type. In Malaysia, the reported durian fruit production in 2013 is estimated at around 320,164 MT.[29] However, only 15%–30% of the entire fruit weight is edible; the remaining parts, including the shell and seeds, are discarded as waste, which causes environmental problems if not properly disposed. The durian shell (DS) consists of 60.5% cellulose, 13.1% hemicellulose and 15.45% lignin.[30] This high cellulosic composition is a very attractive source of value-added products that can be useful in various applications.[31]

The kinetics of DS pyrolysis has not been elucidated. Thus, this work investigates the thermal behaviour and kinetics of DS pyrolysis using non-isothermal TGA at heating rates of 5°C min^{-1}, 10°C min^{-1} and 20°C min^{-1} under nitrogen atmosphere. The kinetic parameters in terms of activation energy and pre-exponential factor are also determined using the Coats-Redfern method with different mechanism models. Statistical analysis was used to determine the best model with the highest correlation coefficient.

2.   EXPERIMENTAL

2.1   Materials

DS sample was collected from a local shop (Nibong Tebal, Penang, Malaysia) and was used as raw material for pyrolysis. The sample was washed three times with adequate distilled water to remove all dust. The sample was dried at 60°C for two days, ground, sieved to a fraction of less than 250 μm particles, and stored in an airtight container before use.

2.2   DS Characteristics

Proximate analysis of DS applied the American Society for Testing and Materials (ASTM) standard E870-82, whereas the ultimate analysis adopted ASTM D3176-89. Sample mass weighed 5 mg, and the N_2 flow rate was 20 ml min^{-1}. The heating rate was kept constant at 20°C min^{-1}. C, H, N, O and S contents were evaluated using an elemental analyser (PerkinElmer 2400 Series II). The characteristics of the DS are shown in Table 1, which reveals the high carbon and low ash contents of DS. Thermal analysis in terms of heating value was conducted with a bomb calorimeter IKA C200 under the standard method (DIN 51900-1). The lignocellulosic composition of the DS sample was evaluated according to the method of Li et al.[32]

Table 1: Characteristics of DS and other biomasses.

Parameter	Biomass					
	Durian shell	Corn straw	Karanj hulls	Rice husk	Cord-grass	Hazelnut husk
Proximate analysis (wt%)						
Moisture	4.96	6.57	3.71	0	9.5	7.24
Ash	3.11	11.8	5.79	16.53	6.2	5.27
Volatiles	70.28	75	84.17	70.6	71.3	73.86
Carbon	21.65	13.21	6.33	12.87	13	20.87
Ultimate analysis (wt%)						
C	42.99	43.83	45.1	39.37	43.9	42.61
H	10.68	5.75	6.13	5.13	6.2	5.51
O	43.13	45.01	48.41	55.18	49.4	50.62
N	2.44	0.97	0	0.32	0.5	1.13
S	0.76	0	0.36	0	0	0.14
Chemical analysis (wt%)						
Cellulose	40.92	36.4	11.73	41.05	34.2	34.5
Hemicellulose	21.99	22.6	47.28	19.05	32.9	20.6
Lignin	25.45	16.6	38.62	14.45	9.6	35.1
Extractives	11.64	7.82	2.37	8.95	23.3	9.8
Thermal analysis (MJ kg^{-1})						
HHV	21.22	–	16.54	16.58	18.5	18.5
Reference	This work	Gai et al.[19]	Islam et al.[22]	Zhang et al.[23]	Liang et al.[24]	Ceylan & Topçu[25]

2.3 TGA Study

Pyrolysis tests of the DS sample were performed using PerkinElmer Pyres TGA1. The temperature-programmed pyrolysis for DS was conducted under a nitrogen atmosphere with a flow rate of 80 ml min^{-1}. A 10 mg sample was inserted directly into a ceramic crucible. The temperature was ramped from 30°C to 900°C in the presence of nitrogen with three heating rates (i.e., 5°C min^{-1}, 10°C min^{-1} and 20°C min^{-1}). Thermogravimetry (TG) and derivative thermogravimetry (DTG) data were processed using instrument software. Each experiment was performed at least twice to confirm repeatability.

2.4 Kinetic Study

2.4.1 Theoretical background

The differential form of the reaction rate equation for the heterogeneous solid-state pyrolysis under a non-isothermal condition can be expressed as:

$$\frac{d\alpha}{dt} = k(T)f(\alpha) \tag{1}$$

where α is the pyrolysis reaction conversion, and $\frac{d\alpha}{dt}$ represents the conversion rate. Equation 2 can be used to calculate α as:

$$a = \frac{W_o - W_t}{W_o - W_\infty} \tag{2}$$

where W_o, W_t and W_∞ refer to the sample weight at the initial state, time t and final state, respectively.

The reaction rate constant represented by $k(T)$ can be expressed by the Arrhenius equation with the form of:

$$k(T) = A\exp\left(-\frac{E_a}{RT}\right) \tag{3}$$

where E_a is the activation energy, A is the pre-exponential factor, R is the gas constant, and T is the pyrolysis temperature. Therefore, Equation 1 can be modified to:

$$\frac{d\alpha}{dt} = A\exp\left(-\frac{E_a}{RT}\right)f(\alpha) \tag{4}$$

The rate of temperature increase per unit time is the heating rate, β, where β = dT/dt = (dT/dα) (dα/dt). Therefore, Equation 4 can be rewritten as:

$$\int_0^\alpha \frac{d\alpha}{f(\alpha)} = g(\alpha) = \frac{A}{\beta}\int_0^T \exp\left(-\frac{E}{RT}\right)dT \tag{5}$$

where $g(\alpha)$ is the integral function of conversion. Equation 5 represents the basic equation, which various models can adopt to analyse the pyrolytic reaction kinetics.

2.4.2 Coats-Redfern method

The Coats-Redfern integral method, which was derived from the Arrhenius equation, was used to analyse the kinetics of DS pyrolysis in this study.[33] This model-fitting method correlates experimental kinetic data based on prior assumptions of the reaction function. The Coats-Redfern equation is given as:

$$ln\left(\frac{g(\alpha)}{T^2}\right) = ln\left(\frac{AR}{\beta E_a}\right) - \frac{E_a}{RT} \qquad (6)$$

The plot of $ln(g(\alpha)/T^2)$ versus $1/T$ is linear after substituting different $g(\alpha)$ values into Equation 6. The corresponding E_a and A values can also be obtained from the slope and the intercept. The common reaction mechanism functions, $g(\alpha)$, are listed in Table 2.

Table 2: Common reaction function forms.[36]

Mechanism	Model	$g(\alpha)$
Reaction order models	First-order R1	$-\ln(1-\alpha)$
	Second-order R2	$(1-\alpha)^{-1} - 1$
	Third-order R3	$[(1-\alpha)^{-2} - 1]/2$
Diffusion models	One-way transport D1	α^2
	Two-way transport D2	$\alpha + [(1-\alpha)\ln(1-\alpha)]$
	Three-way transport D3	$[1 - (1-\alpha)^{1/3}]^2$
	Ginstling-Brounshtein D4	$(1 - 2\alpha/3) - (1-\alpha)^{2/3}$

3.   RESULTS AND DISCUSSION

3.1   Characterisation of the Raw Material

Table 1 shows a comparison of the proximal, elemental and compositional analyses of DS with other biomass wastes. The DS is a high lignocellulosic biomass composed mainly of 40.92% cellulose, 21.99% hemicellulose and 25.45% lignin. The cellulose and hemicellulose biomass contents are generally the main source of volatiles, whereas lignin corresponds to char.[34] These results confirm that pyrolysis of biomass with higher volatile matter content produces higher bio-oil yield.[35] Elemental analysis shows that DS contains 42.99% carbon, 43.13% oxygen, 10.68% hydrogen, 2.44% nitrogen and 0.76% sulphur. Carbon and oxygen, being the most abundant elements, are the main favourable characteristics of lignocellulosic material, which are very attractive for thermal degradation processes.[36] The lower nitrogen and sulphur contents are also important for environmental protection.[37]

Hence, DS, which has a low ash content of 3.11% and high volatile matter of 70.28%, can be considered as an ideal raw material for pyrolysis to produce bio-oil.

3.2   Thermogravimetric Analysis

TG and DTG curves obtained from DS pyrolysis at heating rates of 5°C min^{-1}, 10°C min^{-1} and 20°C min^{-1} are presented in Figures 1 and 2, respectively. The decomposition zone of DS involves three stages (Figure 1). The first stage (59°C–200°C) presented a 4.5% weight loss caused by the release of moisture from the hygroscopic DS and very light volatiles.[38] The main stage (200°C–400°C) displayed a 56% weight loss and indicates cellulose and hemicellulose pyrolysis, as manifested by a strong peak in the 200°C–400°C range in Figure 2.[39] A weak decomposition above 400°C shows a 14% weight loss, which is related to lignin.
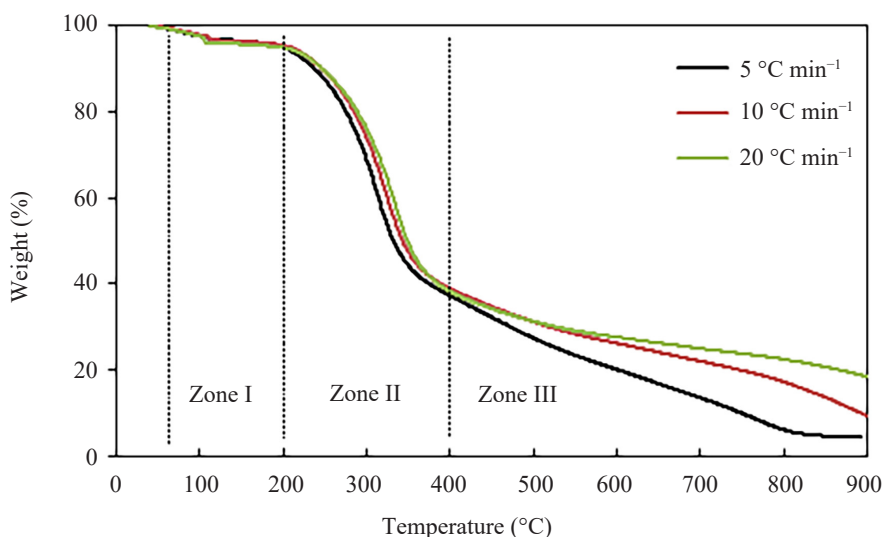

Figure 1: Plot of wt% vs. temperature of DS at different heating rates.

Figures 1 and 2 show the contribution of increasing heating rate to the deceleration of the thermal degradation processes. The high heating rate allowed the sample to reach the given temperature in a short time because of increased thermal lag. The yield of volatile matter decreased slightly with increasing heating rate. The yield is 75.0% at 5°C min^{-1} at a temperature range of 200°C–600°C. This yield decreased significantly to 70.0% and 67.0% at 10°C min^{-1} and 20°C min^{-1}, respectively. The decrease in heating rates only shifted to a lower peak temperature without altering the thermal profile of the decomposition because the heat changing efficiency increased at lower heating rates compared with higher heating rates.

This conclusion is in good agreement with the study by Kim et al., who proposed that the maximum decomposition rate is directly proportional to heating rates because of increasing thermal energy.[40]

In addition, Figure 1 shows that the char yield increased with the heating rate, which could be attributed to the incomplete lignin decomposition under higher heating rate. In Figure 2, a second minor peak appears in the curve of 5°C min^{-1} (temperature range 350°C–450°C), indicating lignin decomposition, although this peak is not obvious in the curves of higher heating rates.[41] Lignin decomposition of lignin can occur across a broad temperature range and this reaction might overlap with hemicellulose degradation at high heating rates.[42]
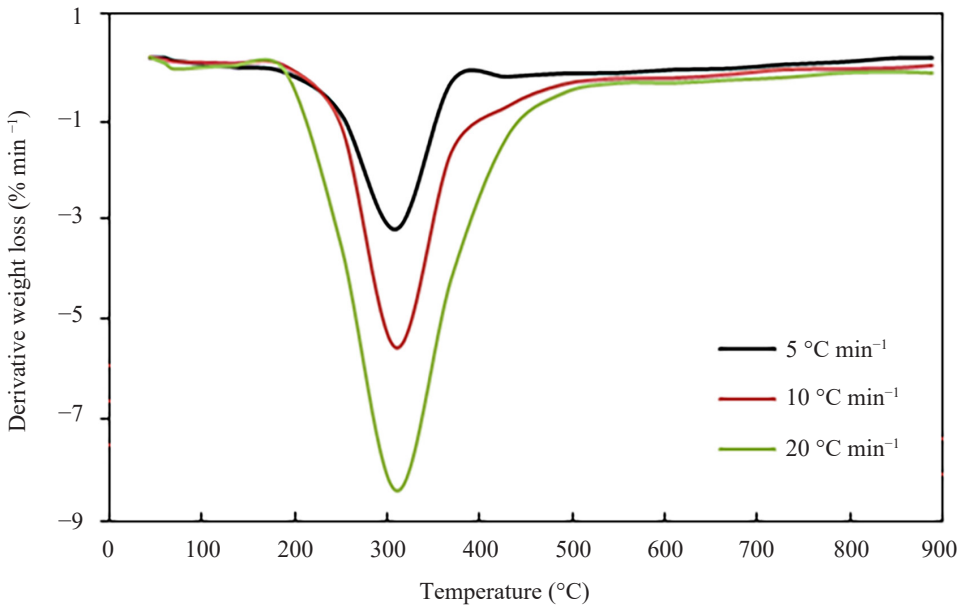

Figure 2: DTG curves of the DS at various heating rates.

Figure 3 shows the change in conversion with temperature for different heating rates in a nitrogen environment. The conversion of the DS sample increased rapidly from 0.1 to 0.8 within the temperature range of 200°C–400°C. Ceylan and Topçu reported the same increase in the conversion hazelnut husk, but within the temperature range of 200°C–600°C.[25] This result may be attributed to the ash content of the hazelnut shell (5.27%) being higher than DS (3.11%).[26]
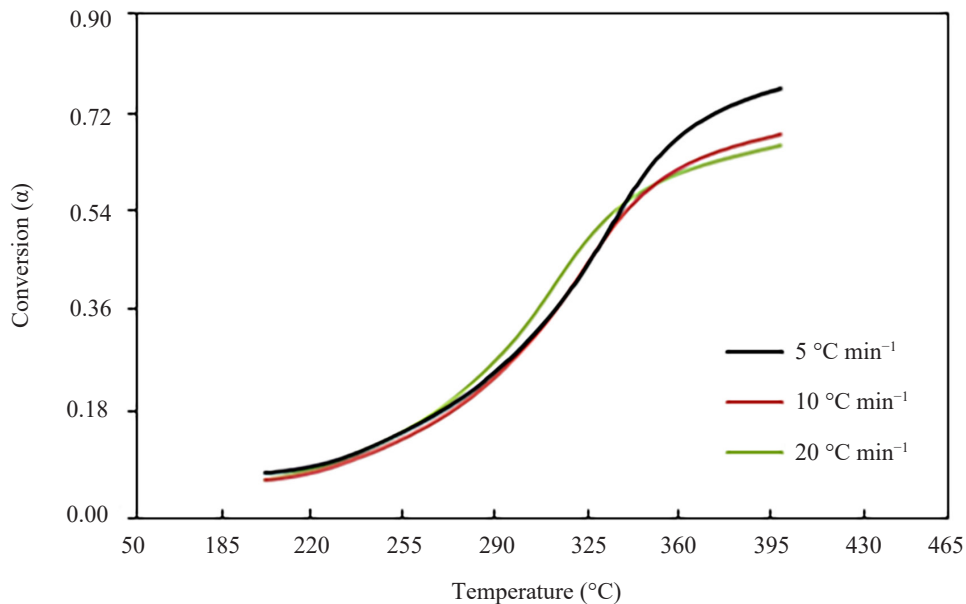
Figure 3: Temperature vs. α of all samples at various heating rates.

3.3   Kinetics Analysis

To understand the kinetics of DS pyrolysis and to evaluate the activation energy and pre-exponential factor, the Coats-Redfern method with different mechanism models was used. Least-squares regression analysis is applied for fitting Equation 6 to the experimental kinetics data of DS pyrolysis. The fitting results in terms of kinetic and statistical parameters within the second stage of decomposition at different heating rates are summarised in Table 3. The first-order (R1), second-order (R2) and third-order (R3) reaction models correlate the kinetic data with average correlation coefficients (R^2) of 0.9895, 0.9833 and 0.9686, respectively. Thus, the R1 reaction model yields the best correlation. The R3 model has a highest average value of activation energy (57.69 kJ mol^{-1}) in comparison with R2 and R1 kinetics at 52.42 kJ mol^{-1} and 48.45 kJ mol^{-1}, respectively. Hence, R3 kinetics is the dominant mechanism of the reaction model kinetics during DS decomposition. According to R3 kinetics, raising the heating rate from 5°C min^{-1} to 20°C min^{-1} increases the activation energy E_a from 41.99 kJ mol^{-1} to 72 kJ mol^{-1} and pre-exponential factor A from 84 min^{-1} to 16899 min^{-1}. This result can be related to the fact that the increase in heating rate decelerates and complicates the decomposition process, so that more activation energy is necessary for driving the reaction.[15] On the other hand, the value of A (min^{-1}) is favourably proportional to E_a (kJ mol^{-1}) according to Equation 6.

Table 3: Coats-Redfern method results of the DS and pyrolysis of other biomasses.

Model	$\beta = 5°C\ min^{-1}$			$\beta = 10°C\ min^{-1}$		
	E_a (kJ mol^{-1})	A (min^{-1})	R^2	E_a (kJ mol^{-1})	A (min^{-1})	R^2
R1	58.99	941.5986	0.9764	42.08	1.06E+01	0.9937
R2	50.03	93.81886	0.9868	50.1	8.48E+01	0.9837
R3	41.99	11.4954	0.9708	59.07	8.40E+01	0.9708
D1	78.99	13168.44	0.9984	77.98	8.43E+03	0.9973
D2	83.39	20133.51	0.9979	82.67	1.37E+04	0.9974
D3	37.18	2.127886	0.9976	36.75	1.73E+00	0.9968
D4	85	6702.249	0.9976	84.4	4.69E+03	0.9973

Model	$\beta = 20°C\ min^{-1}$		
	E_a (kJ mol^{-1})	A (min^{-1})	R^2
R1	44.29	18.96066	0.9984
R2	57.14	458.3997	0.9795
R3	72	16899.6	0.9642
D1	76.67	7053.956	0.9984
D2	83.16	17078.39	0.9977
D3	36.9	1.933353	0.9972
D4	85.61	6846.118	0.9972

The complication of DS pyrolysis and reduction of conversion with increasing heating rate can be also observed from Figure 4 where the elevation of heating rate from 5°C min^{-1} to 20°C min^{-1} for R3 kinetics increases the absolute value of slope from 691 K to 855 K. The activation energies from diffusion kinetic models D1–D4 can also significantly influence DS pyrolysis under nitrogen. The D4 kinetic with the highest average activation energy at 85.0 kJ mol^{-1} significantly affects DS pyrolysis. Although, all mechanism models correlate the kinetics with high R^2 values, the diffusion models, especially the one-way diffusion model D1, show better analysis (average R^2 = 0.9980) than the reaction models (Table 3). However, the reliability of the activation energy values from different kinetics based on their correlation values indicates that DS pyrolysis followed a complex multi-step kinetics to burnout. The kinetic parameters of the Coat-Redfern method for DS were compared with those for *H. verticillata* and karanj hulls.[26,43] The E_a values for DS pyrolysis were lower than those reported for *H. verticillata* and karanj hulls in all of the decomposition models used. This result may be attributed to the low ash content of DS (3.11%) compared with 5.27% and 5.79% for *H. verticillata* and karanj hulls, respectively.[26,43] The presence of high levels of ash in the biomass sample could result in issues in the chemical process, such as fouling, poor pyrolysis and reduced energy conversion efficiency.[24] Moreover, the E_a values

were in the ascending order of DS < karanj hulls < *H. verticillata*. This behaviour may be related to the heating values of three samples, which were 21.22 MJ kg^{-1}, 16.54 MJ kg^{-1} and 14.78 MJ kg^{-1}, respectively.
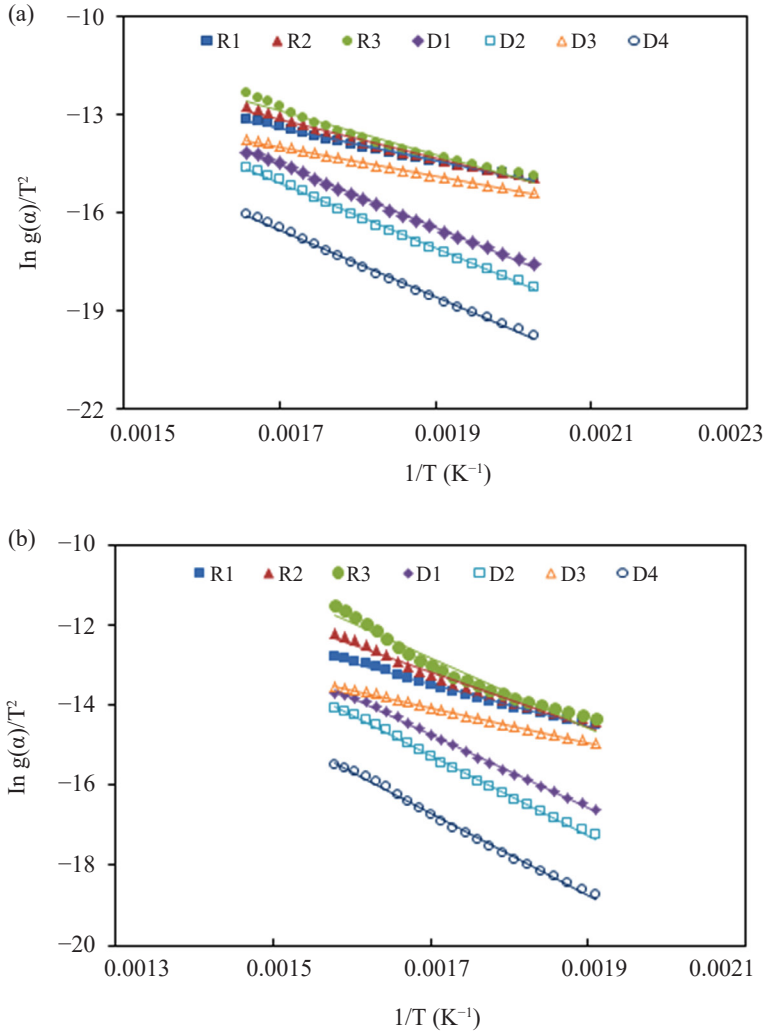

Figure 4: Coats-Redfern plots at (a) β = 5°C min^{-1} and (b) β = 20°C min^{-1}.

4.   CONCLUSION

DS pyrolysis was studied using TGA analysis under nitrogen atmosphere at various heating rates (5°C min^{-1}, 10°C min^{-1} and 20°C min^{-1}). Strong DS pyrolysis is observed in the temperature range of 200°C–400°C, which is a consequence

of hemicellulose and cellulose decomposition. R^2 of 0.991 fits the experimental TGA data using the Coats-Redfern method. Considering the high cellulosic composition and low ash content of DS, the thermochemical system could provide insights into the future application of this biomass as a potential resource of energy and chemicals.

5. ACKNOWLEDGEMENTS

6. REFERENCES

1. Huang, X. et al. (2016). Pyrolysis kinetics of soybean straw using thermogravimetric analysis. *Fuel*, 169, 93–98, https://doi.org/10.1016/j.fuel.2015.12.011.
2. Kim, J. et al. (2017). Pyrolysis of wastes generated through saccharification of oak tree by using CO_2 as reaction medium. *Appl. Therm. Eng.*, 110, 335–345, https://doi.org/10.1016/j.applthermaleng.2016.08.200.
3. Hawash, S. I., Farah, J. Y. & El-Diwani, G. (2017). Pyrolysis of agriculture wastes for bio-oil and char production. *J. Anal. Appl. Pyrol.*, 124, 369–372, https://doi.org/10.1016/j.jaap.2016.12.021.
4. Kabir, G. & Hameed, B. H. (2017). Recent progress on catalytic pyrolysis of lignocellulosic biomass to high-grade bio-oil and bio-chemicals. *Renew. Sust. Energ. Rev.*, 70, 945–967, https://doi.org/10.1016/j.rser.2016.12.001.
5. Fadhil, A. B., Ahmed, A. I. & Salih, H. A. (2017). Production of liquid fuels and activated carbons from fish waste. *Fuel*, 187, 435–445, https://doi.org/10.1016/j.fuel.2016.09.064.
6. Sharma, A., Pareek, V. & Zhang, D. (2015). Biomass pyrolysis: A review of modelling, process parameters and catalytic studies. *Renew. Sust. Energ. Rev.*, 50, 1081–1096, https://doi.org/10.1016/j.rser.2015.04.193.
7. Magdziarz, A. & Werle, S. (2014). Analysis of the combustion and pyrolysis of dried sewage sludge by TGA and MS. *Waste Manage.*, 34, 174–179, https://doi.org/10.1016/j.wasman.2013.10.033.
8. Foo, K. Y. & Hameed, B. H. (2012). Textural porosity, surface chemistry and adsorptive properties of durian shell derived activated carbon prepared by microwave assisted NaOH activation. *Chem. Eng. J.*, 187, 53–62. https://doi.org/10.1016/j.cej.2012.01.079.
9. Foo, K. Y. & Hameed, B. H. (2012). Porous structure and adsorptive properties of pineapple peel based activated carbons prepared via microwave assisted KOH and K_2CO_3 activation. *Micropor. Mesopor. Mat.*, 148, 191–195, https://doi.org/10.1016/j.micromeso.2011.08.005

10.　Njoku, V. O. & Hameed, B. H. (2011). Preparation and characterization of activated carbon from corncob by chemical activation with H_3PO_4 for 2,4-dichlorophenoxyacetic acid adsorption. *Chem. Eng. J.*, 173, 391–399, https://doi.org/10.1016/j.cej.2011.07.075.

11.　Collazzo, G. C. et al. (2017). A detailed non-isothermal kinetic study of elephant grass pyrolysis from different models. *Appl. Therm. Eng.*, 110, 1200–1211, https://doi.org/10.1016/j.applthermaleng.2016.09.012.

12.　Moralı, U. & Sensöz, S. (2015). Pyrolysis of hornbeam shell (*Carpinus betulus* L.) in a fixed bed reactor: Characterization of bio-oil and bio-char. *Fuel*, 150, 672–678, https://doi.org/10.1016/j.fuel.2015.02.095.

13.　Huang, X. (2014). Influences of pyrolysis conditions in the production and chemical composition of the bio-oils from fast pyrolysis of sewage sludge. *J. Anal. Appl. Pyrol.*, 110, 353–362, https://doi.org/10.1016/j.jaap.2014.10.003.

14.　Liu, G. et al. (2016). Thermal behavior and kinetics of municipal solid waste during pyrolysis and combustion process. *Appl. Therm. Eng.*, 98, 400–408, https://doi.org/10.1016/j.applthermaleng.2015.12.067.

15.　Fernandez, A. et al. (2016). Kinetic study of regional agro-industrial wastes pyrolysis using non-isothermal TGA analysis. *Appl. Therm. Eng.*, 106, 1157–1164, https://doi.org/10.1016/j.applthermaleng.2016.06.084.

16.　Boon, T. H. et al. (2017). Thermogravimetric study of napier grass in inert and oxidative atmospheres conditions. *J. Phys. Sci.*, 28, 155–169, https://doi.org/10.21315/jps2017.28.s1.10.

17.　Nyakuma, B. B. et al. (2016). Combustion kinetics of Shankodi-Jangwa coal. *J. Phys. Sci.*, 27, 1–12, https://doi.org/10.21315/jps2016.27.3.1

18.　Wu, W. et al. (2015). Kinetics and reaction chemistry of pyrolysis and combustion of tobacco waste. *Fuel*, 156, 71–80, https://doi.org/10.1016/j.fuel.2015.04.016.

19.　Gai, C., Dong, Y. & Zhang, T. (2013). The kinetic analysis of the pyrolysis of agricultural residue under non-isothermal conditions. *Bioresour. Technol.*, 127, 298–305, https://doi.org/10.1016/j.biortech.2012.09.089.

20.　Ouyang, W. et al. (2015). Optimisation of corn straw biochar treatment with catalytic pyrolysisin intensive agricultural area. *Ecol. Eng.*, 84, 278–286, https://doi.org/10.1016/j.ecoleng.2015.09.003.

21.　Jaroenkhasemmeesuk, C. & Tippayawong, N. (2016). Thermal degradation kinetics of sawdust under intermediate heating rates. *Appl. Therm. Eng.*, 103, 170–176, https://doi.org/10.1016/j.applthermaleng.2015.08.114.

22.　Islam, M. A., Asif, M. & Hameed, B. H. (2015). Pyrolysis kinetics of raw and hydrothermally carbonized Karanj (*Pongamia pinnata*) fruit hulls via thermogravimetric analysis. *Bioresour. Technol.*, 179, 227–233, https://doi.org/10.1016/j.biortech.2014.11.115.

23.　Zhang, S. et al. (2016). Effects of water washing and torrefaction on the pyrolysis behavior and kinetics of rice husk through TGA and Py-GC/MS. *Bioresour. Technol.*, 199, 352–361, https://doi.org/10.1016/j.biortech.2015.08.110.

24.　Liang, Y. et al. (2014). Thermal decomposition kinetics and characteristics of Spartina alterniflora via thermogravimetric analysis. *Renew. Energy*, 68, 111–117, https://doi.org/10.1016/j.renene.2014.01.041.

25.   Ceylan, S. & Topçu, Y. (2014). Pyrolysis kinetics of hazelnut husk using thermogravimetric analysis. *Bioresour. Technol.*, 156, 182–188, https://doi.org/10.1016/j.biortech.2014.01.040.

26.   Hu, Z. et al. (2015). Characteristics and kinetic studies of *Hydrilla verticillata* pyrolysis via thermogravimetric analysis. *Bioresour. Technol.*, 194, 364–372, https://doi.org/10.1016/j.biortech.2015.07.007.

27.   Amid, B. T. & Mirhosseini, H. (2012). Optimisation of aqueous extraction of gum from durian (*Durio zibethinus*) seed: A potential, low cost source of hydrocolloid. *Food Chem.*, 132, 1258–1268, https://doi.org/10.1016/j.foodchem.2011.11.099.

28.   Foo, K. Y. & Hameed, B. H. (2012). Textural porosity, surface chemistry and adsorptive properties of durian shell derived activated carbon prepared by microwave assisted NaOH activation. *Chem. Eng. J.*, 187, 53–62, https://doi.org/10.1016/j.cej.2012.01.079.

29.   Manshor, M. R. et al. (2014). Mechanical, thermal and morphological properties of durian skin fibre reinforced PLA biocomposites. *Mater. Des.*, 59, 279–286, https://doi.org/10.1016/j.matdes.2014.02.062.

30.   Masrol, S. R., Ibrahim, M. H. I. & Adnan, S. (2015). Chemi-mechanical pulping of durian rinds. *Proced. Manuf.*, 2, 171–180, https://doi.org/10.1016/j.promfg.2015.07.030.

31.   Abidina, M. A. Z. et al. (2011). Recovery of gold (III) from an aqueous solution onto a *Durio zibethinus* husk. *Biochem. Eng. J.*, 54, 124–131, https://doi.org/10.1016/j.bej.2011.02.010.

32.   Li, S. et al. (2004). Fast pyrolysis of biomass in free-fall reactor for hydrogen-rich gas. *Fuel Process. Technol.*, 85, 1201–1211, https://doi.org/10.1016/j.fuproc.2003.11.043.

33.   Coats, A. W. & Redfern, J. P. (1964). Kinetic parameters from thermogravimetric data. *Nature*, 201, 68–69, https://doi.org/10.1038/201068a0.

34.   Akhtar, J. & Amin, N. S. (2012). A review on operating parameters for optimum liquid oil yield in biomass pyrolysis. *Renew. Sust. Energ. Rev.*, 16, 5101–5109, https://doi.org/10.1016/j.rser.2012.05.033.

35.   Kan, T., Strezov, V. & Evans, T. J. (2016). Lignocellulosic biomass pyrolysis: A review of product properties and effects of pyrolysis parameters. *Renew. Sust. Energ. Rev.*, 57, 1126–1140, https://doi.org/10.1016/j.rser.2015.12.185.

36.   White, J. E., Catallo, W. J. & Legendre, B. L. (2011). Biomass pyrolysis kinetics: A comparative critical review with relevant agricultural residue case studies. *J. Anal. Appl. Pyrol.*, 91, 1–33, https://doi.org/10.1016/j.jaap.2011.01.004.

37.   Tripathi, M., Sahu, J. N. & Ganesan, P. (2016). Effect of process parameters on production of biochar from biomass waste through pyrolysis: A review. *Renew. Sust. Energ. Rev.*, 55, 467–481, https://doi.org/10.1016/j.rser.2015.10.122.

38.   Jun, T. Y. et al. (2010). Effect of activation temperature and heating duration on physical characteristics of activated carbon prepared from agriculture waste. *Environ. Asia*, 3, 143–148.

39.   Yang, H. et al. (2007). Characteristics of hemicellulose, cellulose and lignin pyrolysis. *Fuel*, 86, 1781–1788, https://doi.org/10.1016/j.fuel.2006.12.013.

40.   Kim, S. S. et al. (2013). Thermogravimetric characteristics and pyrolysis kinetics of *Alga sagarssum* sp. biomass. *Bioresour. Technol.*, 139, 242–248, https://doi.org/10.1016/j.biortech.2013.03.192.

41.   Manyà, J. J., Velo, E. & Puigjaner, L. (2003). Kinetics of biomass pyrolysis: A reformulated three-parallel-reactions model. *Ind. Eng. Chem. Res.*, 42, 434–441, https://doi.org/10.1021/ie020218p.

42.   Santos, K. G. et al. (2012). Sensitivity analysis applied to independent parallel reaction model for pyrolysis of bagasse. *Chem. Eng. Res. Des.*, 90, 1989–1996, https://doi.org/10.1016/j.cherd.2012.04.007.

43.   Islam, M. A. et al. (2016). A thermogravimetric analysis of the combustion kinetics of karanja (*Pongamia pinnata*) fruit hulls char. *Bioresour. Technol.*, 200, 335–341, https://doi.org/10.1016/j.biortech.2015.09.057.